DELIVERABLE 1. NUMERICAL ANALYSIS OF THE USE OF DIFFERENT REFRIGERANTS IN THE HEAT PUMP TO INSTALL IN THE SWIMMING POOL FACILITY

Research project: Design and evaluation of descarbonisation strategies to achieve near zero emissions indoor swimming pools assisted by renewable energies – nZEPools (TED2021-131173B-I00)

Financed by the Ministry of Science and Innovation, Spain and the support of the European Regional Development Fund and NextGenerationEU Fund

M.A. Tortosa-Saorín, F. Illán-Gómez, J.R. García-Cascales, F.J. Sánchez-Velasco, R.E. Biyogo Obono

Last updated. 2025-01-30

1. Introduction

This study is carried out as part of a research project in which the performance of an air-to-water heat pump operating with different refrigerants is analyzed. With the help of the refrigeration plant regulations, we are going to look for A1 type refrigerants, since they are the safest refrigerants as they are non-toxic and non-flammable. In addition, we will constrict it to refrigerants with a global warming potential (GWP) lower than 150 that can be used in heat pump applications for heating swimming pools and generating DHW (low/medium temperature). This limit has been chosen based on the 2024 F-Gas regulations, which establish bans on the marketing of equipment based on the GWP or the refrigerant they use. Although this regulation does not affect an installation such as the one we have designed, we have considered this limit for the type of refrigerants that the regulation considers as the low GWP ones.

2. Refrigerant selection

As a result of this study, the refrigerants included in the current regulation were analyzed, revealing that only three in the A1 category have a global warming potencia (GWP) below 150: CO_2 (R744), R471A and R1233zd(E). However, R1233zd(E) was excluded due to its low-pressure characteristics, which make it more suitable for high-temperature heat pump applications. Under normal evaporation conditions, this refrigerant operates at pressures below atmospheric pressure, posing a risk in the event of leaks, as air and moisture could enter the circuit instead of refrigerant escaping. This behavior is undesirable since the aim is generally to operate the entire circuit at pressures above atmospheric pressure.

For instance, the saturation pressures of R1233zd(E) at different temperatures are notably low: at -5ºC, 0.38 bar; at +20ºC, 1.08 bar; at +50ºC, 2.93 bar; at +90ºC, 8.33 bar; and at +130ºC, 19.1 bar. These characteristics reinforce its unsuitability for this case.

Therefore, the study will focus on the comparative analysis of two systems using the refrigerants CO_2 and R471A, both suitable for operating under appropriate pressure conditions and capable of partially meeting the needs of the indoor swimming pool located in La Aljorra, Cartagena, Spain. Although our proposal is to study these two refrigerants, we have found some difficulties to characterize the thermodynamic states of R471A. To circumvent this, we have used the properties of R1234ze(e) whose utilization is justified in the following section.

3. Justification for the use of R1234ze(e) instead of R471A for this analysis

In this study, various potential refrigerants whose physicochemical properties are similar to those of R471A are considered. Namely, refrigerants R124, R513A, R1234ze(E), and R471A are evaluated. From this comparison (Figure 1), it is identified that R1234ze(E) has thermodynamic and transport properties very similar to those of R471A, and unlike the latter, it is supported by major equipment selection software used by manufactures: compressors (BITZER), condensers (SWEP), and evaporators (GUTNER). For this reason, R1234ze(E) is chosen as the basis for equipment selection and system modeling.

The direct use of R471A presents multiple practical limitations. Although, in theory, the equipment selected for R1234ze(E) could be valid for R471A due to their similarities, R471A is an azeotropic mixture that includes substances such as R1336mzz(E), which is not available in the CoolProp databases (used in TRNSYS) or in the official version of REFPROP (used in MATLAB). Although an experimental file with the properties of R1336mzz(E) for REFPROP has been found, the lack of certainty about its accuracy and its incompatibility with TRNSYS complicates its use in simulations.

Additionally, equipment selection with R471A faces significant challenges. Currently, there is no software available for selecting evaporators and condensers with this refrigerant. Regarding compressors, the only identified manufacturer, BOCK, provides limited information and only for a discontinued model (HG4/310-4), which has been replaced by the HG34e/315-4, for which no data is available for R471A. These limitations reinforce the need to use an alternative refrigerant for the design and modeling phases.

The study concludes that, although the final refrigerant in the application will be R471A, the system design and modeling will be carried out using R1234ze(E). This refrigerant exhibits very similar behavior to R471A, as shown in the graphs in Figures 1-7. This approach allows leveraging available design tools and overcoming the practical limitations associated with the direct use of R471A.

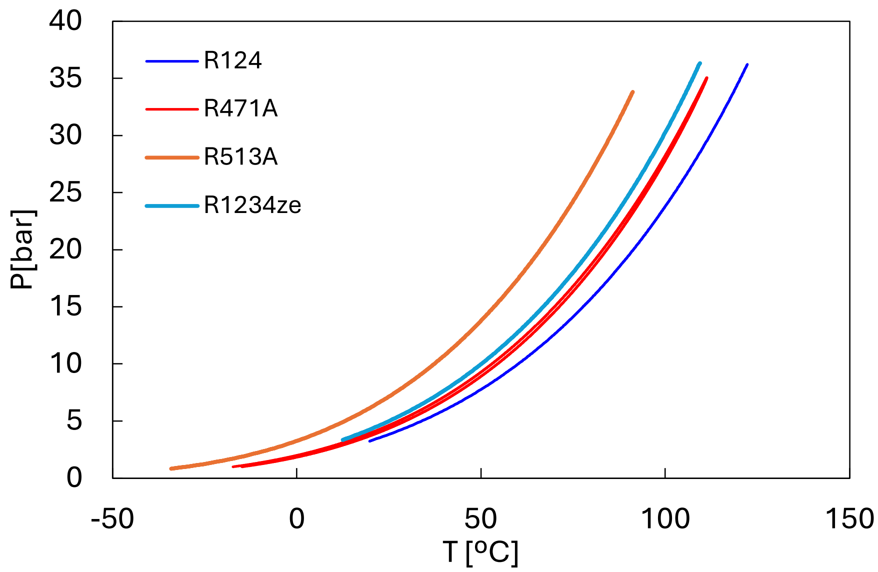

Figure 1. Refrigerants with similar behaviour

The following graphs compare the specific volume (Figure 2), thermal conductivity (Figure 3) and viscosity (Figure 4) of the refrigerants R471A and R1234ze(E) for the vapor phase and for the liquid phase.

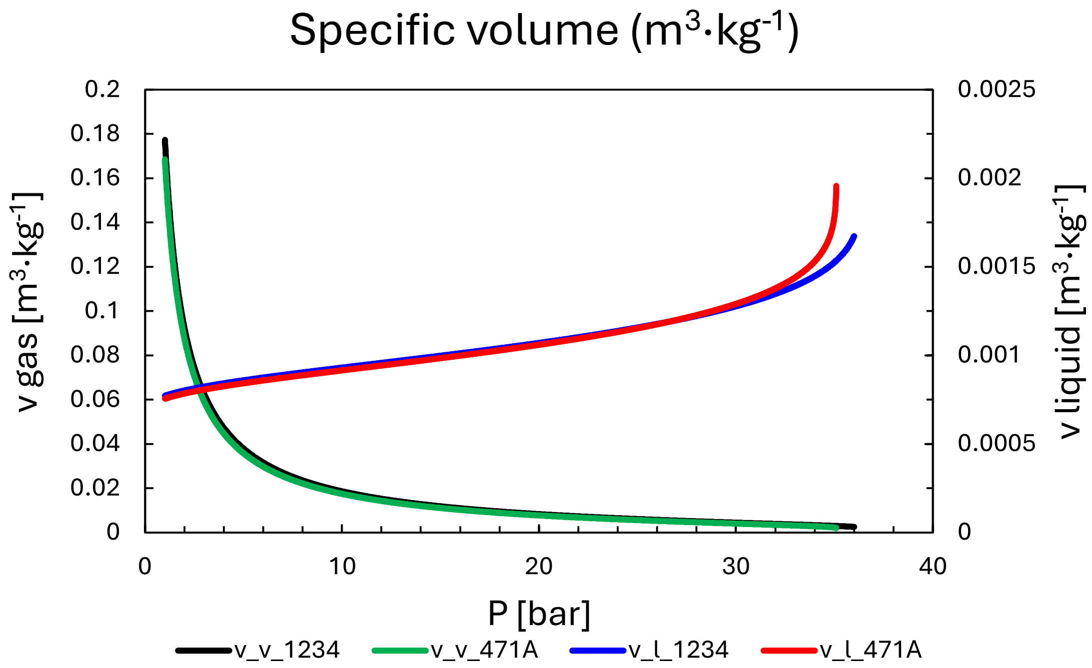

Figure 2. Specific volume of different refrigerants

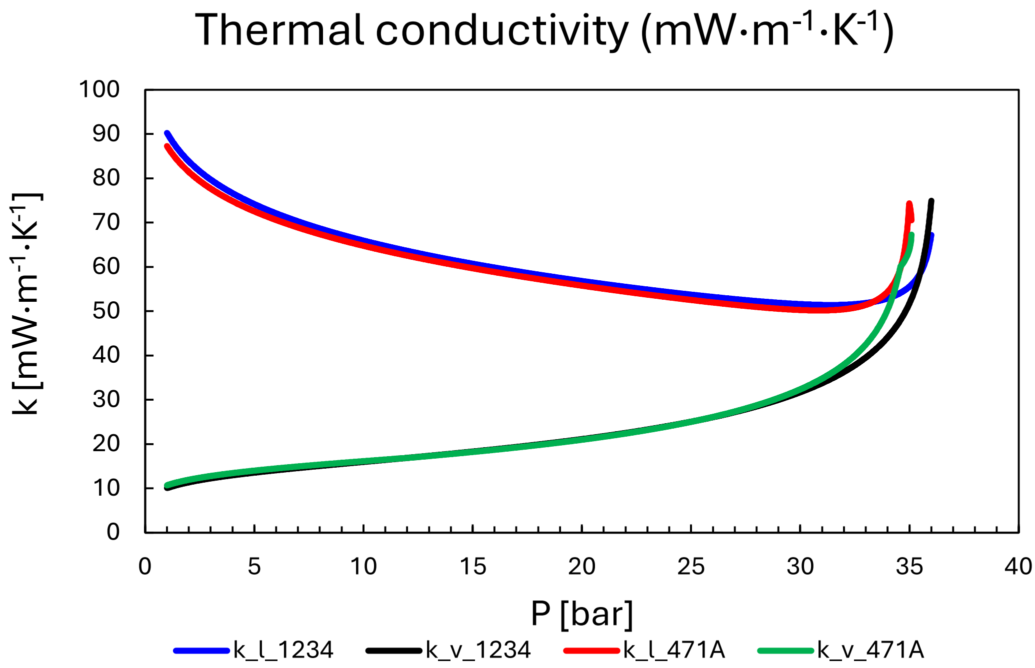

Figure 3. Thermal conductivity of the different refrigerants

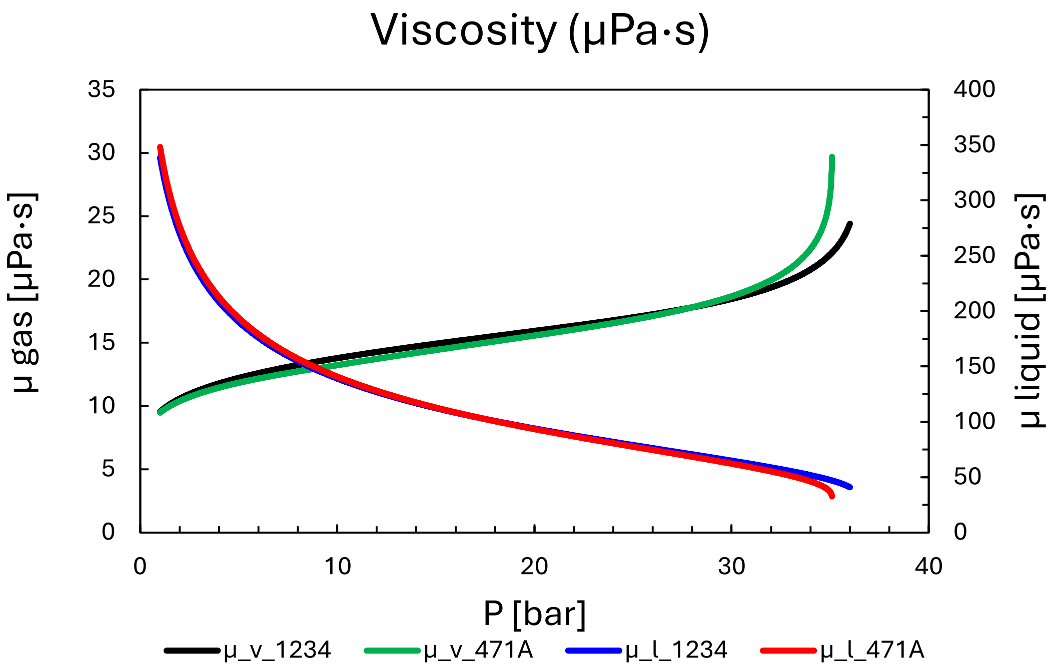

Figure 4. Viscosity of the different refrigerants

So, we conclude that R1234ze(E) is very similar by comparing the relationship between their thermodynamic properties as can be seen in the graphs from Figure 5 to Figure 7:

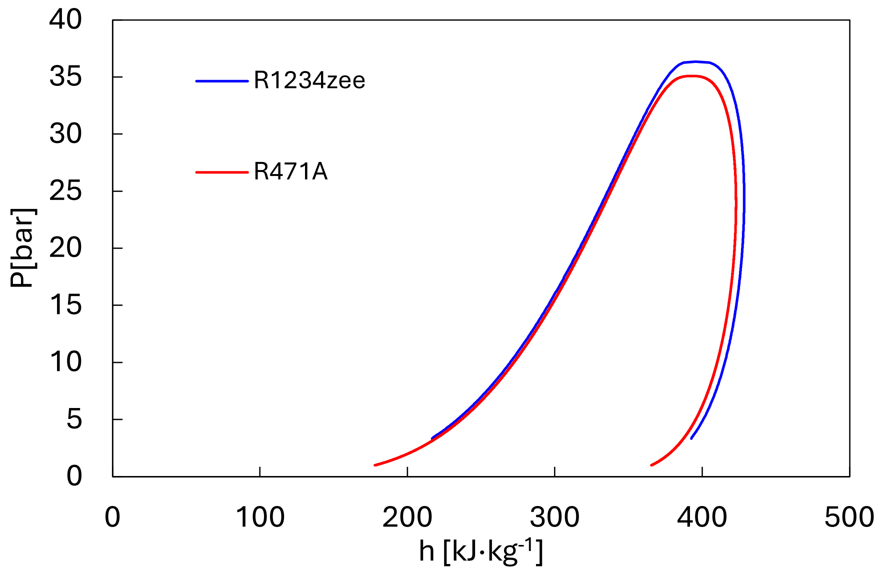

Figure 5. Thermodynamic properties

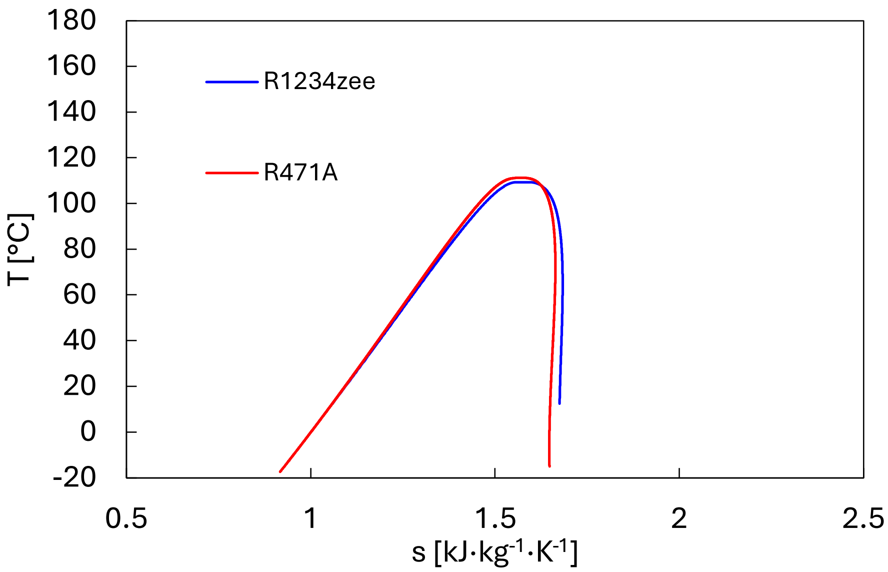

Figure 6. Thermodynamic properties

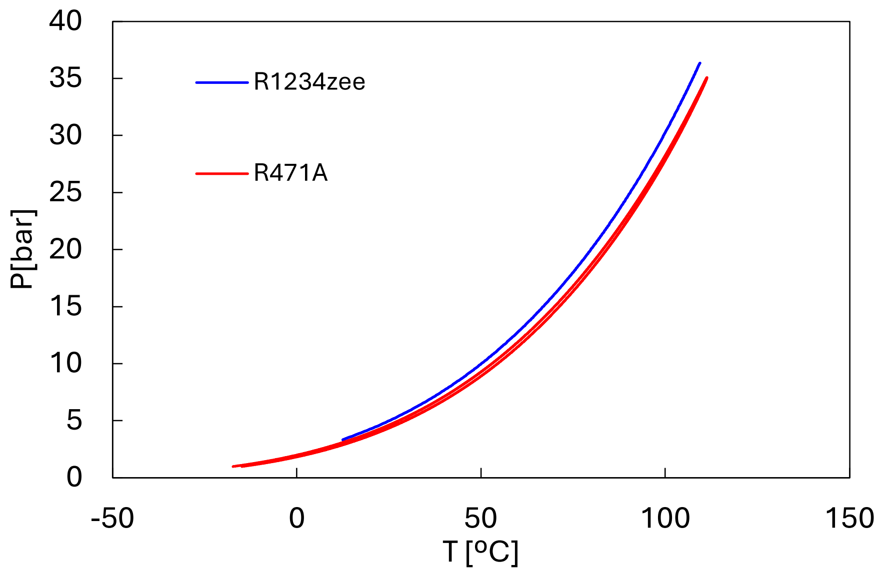

Figure 7. Thermodynamic properties

4. Analysis differences CO_2-R1234ze(E). As mentioned above, our aim is to see the differences between the use of two A1 refrigerants with a GWP of less than 150 in a heat pump, specifically CO_2 and R1234ze(E). To carry out this comparison it is necessary to design two heat pumps with similar characteristics.

The aim of the analysis in Table 1 is to select a R1234ze(E) compressor model that has a similar power output to the CO_2 compressor already chosen, considering different operating conditions. For this purpose, we use Bitzer software, which provides the corresponding power outputs for each model under a condensing temperature of 35ºC.

Initially, it is considered to select a compressor for R1234ze(E) that delivers the same power as the CO_2 system under the most unfavorable conditions studied, corresponding to an evaporating temperature of -5°C. However, it is observed that, when sizing the compressor under these conditions, the heating capacity of the system with R1234ze(E) increases significantly in conditions of higher evaporating temperature, such as in summer (20°C), considerably exceeding the power of the CO_2 system.

This appears to be due to a greater variation in saturation pressure as the evaporation temperature changes, which is associated with a larger variation in fluid density and, therefore, a greater variation in the refrigerant flow rate.

To address this discrepancy, a different strategy is adopted: select a compressor for R1234ze(E) that provides a power similar to that of CO_2 at an intermediate operating point, corresponding to an evaporating temperature of 7.5°C.

Based on this decision, power variations between both systems are analyzed under the extreme conditions studied (-5 °C and 20 °C) to evaluate how the performance of each refrigerant varies under these situations.

Table 1. **Differences CO_2-R1234ze(E).**

	P_{evap} (bar)		ρ ($kg \cdot m^{-3}$)		Q_{cond} (kW)		COP (-)	
T_{evap} (°C).	CO_2	R1234ze(E)	CO_2	R1234ze(E)	CO_2	R1234ze(E)	CO_2	R1234ze(E)
-5	39.6946525	1.7942312	104.534625	9.4858985	23.0484409	14.6731535	4.86455758	4.41673838
7.5	42.2954902	2.83037678	112.607066	14.6514201	24.4792647	23.7778537	5.32460163	6.35579447
20	57.2905258	4.27342777	164.235483	21.5126226	33.6409996	35.8784801	8.82712982	8.62428849
Var. 1-2 (%)	7%	58%	8%	54%	6%	62%	9%	44%
Var. 1-3 (%)	44%	138%	57%	127%	46%	145%	81%	95%

5. Description/Design/Selection of components for the System with R1234ze(e) and modeling of the system with IMST-ART

In this section we will develop the description, design and selection of components with R1234ze(E) and the modeling of the system with IMS-ART. In deliverable 4 you can find all this information for the heat pump that will be used as CO_2 refrigerant.

5.1. Compressor

As there is a big difference in power between summer (T_{evap}=-+20°C) and winter (T_{evap}=-5°C), we will make the selection to give a similar power to the CO_2 compressor at an intermediate evaporating temperature (7.5°C).

There are 2 possible models, the 4BES-9Y-40S, which gives 23.7 kW and the 4TES-9Y-40P which gives 27.9 kW, we will choose the 2nd one (Figure 8).

Figure 8. Bitzer compressor, model 4TES-9Y-40P

Its characteristics are given in Table 2.

Table 2. Technical characteristics of the compressor.

Displacement (1450rpm 50Hz)	41.33 m^3/h
Oil charge	2.60 L
Motor voltage (more on request)	380-420V Y-3-50Hz
Max. operating current	19.9 A
Max. power input	13.0 kW

5.2. Evaporator

First, we obtain the conditions used to select the evaporator, which corresponds to the power provided by the compressor for an intermediate evaporation temperature. Based on these design conditions, and using Güntner's online software, the corresponding model was obtained. Table 3 summarizes the design conditions considered.

Table 3. Evaporator design conditions

Capacity	23.40 kW
Air Flow	8684 m^3/h
Air inlet	18º C
Evaporation temperature	7.5º C
Superheating	7 K
Condensation temperature	35º C

According to the design conditions, the evaporator selected for this installation is a 'Güntner GACC PX 040.1/31N/HJA7A.UNNN' (Figure 9).

Figure 9. Güntner evaporator.

According to Figure 10 view, evaporator dimensions are as follows:

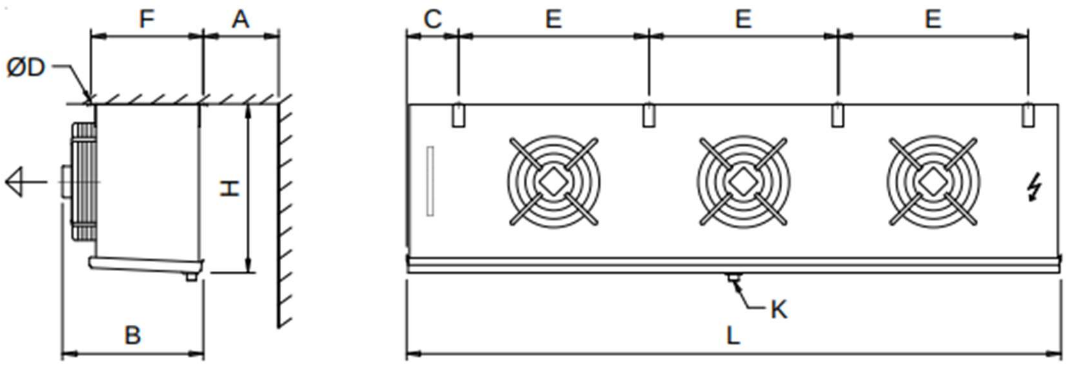

Figure 10. Güntner evaporator schematic.

L =2366mm B =560mm H =565mm E =680mm F =406mm C =177mm
A =400mm D =11mm K=G1$_{1/4"}$

Its general characteristics are as shown in Table 4:

Table 4. General evaporator characteristics

Exchange surface	58.70 m^2
Tube volume	19.2 L
Fin pitch	7 mm
Number of pitches	8
Distributions	10

5.3. Condenser

As with the evaporator, Table 5 shows the conditions used to design the plate heat exchanger we are going to use as condenser. These correspond to the case in which evaporation temperature is 7.5ºC. To do so, we use SWEP's online selection software which is fed with these conditions, the most suitable solution provided is the selected model.

Table 5. Design conditions for 'Swep 26'.

	R1234ze(E)	Water
Inlet Temperature [ºC]	49.90	28.00
Outlet Temperature [ºC]	35.09	32.82
Flow rate [kg/s]	0.16083	1.389

According to the design conditions, a 'SWEP B26' has been selected to model the condenser (Figure 11a). Their dimensions according to the schematic view of Figure 11b are gathered in Table 6. The pitch is 1.61 mm.

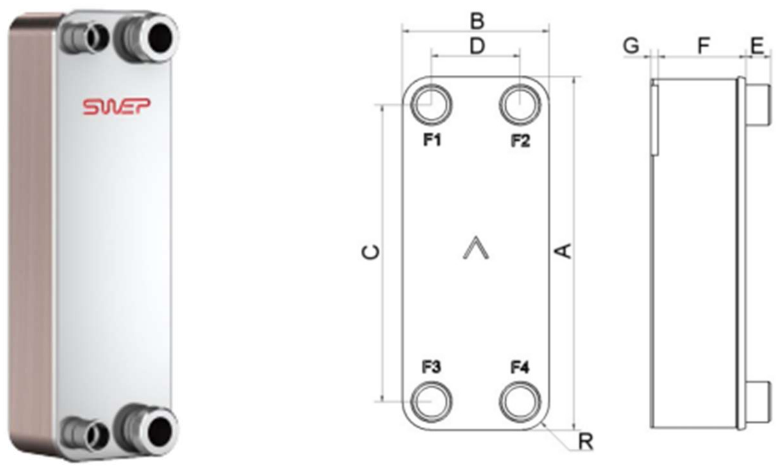

a) b)

Figure 11. Swep B26 plate heat exchanger.

Table 6. Plate heat exchanger dimensions.

	Dimensions [mm]
A	376
B	119
C	329
D	72

The selected plate exchanger has an exchange surface of 2.30 m^2. In addition, the overall heat transfer coefficient (OHTC) for this gas cooler has a value of 2690 W/ m^2.

6. Model description

The model description for R1234ze(E) is explained below. Deliverable 2 is dedicated to model description for CO_2.

For the development of the model, the compressor has been modeled using the polynomials provided by the manufacturer, while the heat exchangers have been modeled through correlations from a least squares adjustment carried out with Matlab. This adjustment has been based on operating points of the pump, determined within the input variables ranges that correspond to the expected operating conditions in the pool. These operating points were obtained by modelling each of the components using IMST-ART.**6.1. Compressor**

The component created in TRNSYS to characterise the compressor has been carried out by considering the polynomials provided by the manufacturer according to AHRI standard 540 which has the general expression

$$y = c_1 + c_2\, t_o + c_3\, t_c + c_4\, {t_o}^2 + c_5\, t_o\, t_c + c_6\, {t_c}^2 + c_7\, {t_o}^3 + c_8\, t_c\, {t_o}^2 + c_9\, t_o\, {t_c}^2 + c_{10}\, {t_c}^3$$

where t_o is the evaporation temperature, t_c is the condensation temperature and the coefficients (c_0 to c_9) are polynomial adjustment coefficients whose values depend on the variables of interest calculated with the expression. In this case, the power absorbed by the compressor and the mass flow rate. In Table 7, the coefficients needed to determine these variables are gathered.

Table 7. Polynomial coefficient of the compressor 4TES-9Y-40P according to AHRI 540.

	$\dot{W}$ [W]	$\dot{m}_r$ [kg/s]
c_1	1723.09345	0.12565114
c_2	-86.8394207	0.00520434
c_3	69.6461264	-6.0584E-05
c_4	-2.90052101	7.846E-05
c_5	4.28185651	-9.3084E-06
c_6	-0.04657875	-4.1884E-06
c_7	-0.03314575	4.184E-07
c_8	0.04140998	-2.7589E-07
c_9	-0.01395839	3.1969E-10
c_{10}	-0.00282738	-2.0227E-08

Once these variables are estimated, the output variables of the model are obtained taking into account the input variables are inlet enthalpy, the condensation temperature and the evaporation temperature, so the outlet enthalpy is

$h_{ro} = h_{ri} + \dot{W}/\dot{m}_r$In addition to those already mentioned, other output variables we obtain are the refrigerant's outlet pressure and temperature.

Thermodynamics properties are determined by means of CoolProp subroutines which are available with TRNSYS 18 program.

6.2. Evaporator

To characterize this evaporator, the IMST-ART software has been used, which requires the geometrical data of the heat exchanger in Table 8.

Table 8. Geometrical data of the heat exchanger

General Dimensions	
Exchanger Width [m]	2.08
Longit. Spacing [mm]	50
Trans. Spacing [mm]	50
Tube Data	
Tube Material	Copper
Outer Diameter [mm]	12.70
Thickness [mm]	0.813
Inner Surface	Smooth
Fin Data	
Thickness [mm]	0.1
Fin Pitch [mm]	7
Type	Louvered
Material	Aluminium

The evaporator model used in the cycle has been initially developed by using IMST-ART software, adapted to characterize its behavior as a function of various operating conditions. This software is fed with a set of input variables representing the actual system conditions. The selection of these input conditions is carefully done, to avoid operating points that the program cannot solve due to its limited design for subcritical cycles.

The air inputs are its inlet conditions which are defined by three main variables: air temperature, relative humidity, and volumetric flow rate, the latter constant at 8684 m^3/h, a value corresponding to the nominal flow rate of the evaporator. To represent realistic operating conditions, these variables are adjusted according to different climatic scenarios. During winter, low temperatures (from -5 ºC to 20ºC) with high relative humidity (around 80 %) are simulated, while in summer air temperatures up to 35 ºC and relative humidity levels between 40 % and 58.75 % are considered. This variability in air conditions allows the evaluation of the evaporator efficiency over a wide range of typical operating situations.

Regarding the refrigerant inputs, the condensation temperature and the mass flow rate are the variable supplied to the program, the latter is obtained considering the polynomial provided by the compressor manufacturer according to AHRI 540 standard. Regarding the relationship between air temperature and condensation temperature, the correlation $T_c = 1.090909 * T_{air} + 16.78182$ has been obtained, taking into account that the condensation temperature at 35ºC increased from an air temperature of 16.7 ºC on. For superheating, specific values of 3, 6, 9 and 12 K were used, allowing a parametric analysis of the system.

In conclusion, the modeling process is based on an accurate selection of input conditions for IMST-ART, setting parameters and applying filters on the air and refrigerant variables. This allows simulating the evaporator behavior and obtaining results from the evaporator.

To model the evaporator component in TRNSYS, correlations and coefficients (Table 9) have been generated with MATLAB using the results obtained by IMST-ART (total pressure drop and saturation temperature at the refrigerant outlet) together with the input conditions introduced in it. Correlations are obtained for the total pressure drop (Δpr) and for the evaporation pressure (P_{ro}).

$$\Delta p_r = c_0 + c_1 T_{seci} + c_2\, HR + c_3\, T_{cond} + c_4 \dot{m}_{ri} + c_5\, SH + c_6\, T_{seci}^2 + c_7 \dot{m}_{ri}^2$$

$$P_{ro} = c_0 + c_1\, T_{seci} + c_2\, HR + c_3 T_{cond} + c_4 \dot{m}_{ri} + c_5\, SH + c_6\, T_{seci}^2 + c_7\, HR^2 + c_8 \dot{m}_{ri}^2$$

These are the correlations obtained and Table 9 shows the coefficients used for each variable.

Table 9. Evaporator coefficients

	P_{ro} [Pa]	Δp_r [Pa]
c_0	-15557	-4058.4
c_1	6223.5	-446.18
c_2	4254.4	-94.201
c_3	444.65	81.752
c_4	11.7	59.639
c_5	-3030	341.97
c_6	104.87	-7.4595
c_7	-24.5	2.28E-02
c_8	-0.127	

The refrigerant inlet pressure is calculated as $P_{ri} = P_{ro} + \Delta p_r$

The evaporation temperature and the refrigerant's outlet enthalpy are obtained using the properties from the CoolProp subroutine available in TRNSYS 18. The refrigerant's outlet enthalpy is obtained using the saturation temperature at outlet pressure plus the superheat. Finally, the total power is calculated by the following expression:

$$Q_t = m_{ri} * (h_{ro} - h_{ri})$$

6.3. Condenser

To characterize the condenser, the IMST-ART software has been used, which requires the geometrical data of the heat exchanger in Table 10:

Table 10. Geometrical data of the heat exchanger

Geometry	
HPCD	0.072 m
VPCD	0.329 m
Port Diameter (PD)	18 mm
Plate Pitch (PP)	1.33 mm
Plate Thickness	0.35 mm
Channel Type	M
Area EnhF	1.17

The condenser model used in this cycle has been modeled using IMST-ART software, adapted to characterize its behavior as a function of various operating conditions. This software is fed with a set of input variables representing the actual system conditions. The selection of these input conditions is done carefully, in order to avoid operating points that the program cannot solve due to its limited design for subcritical cycles.

Water inlet conditions are defined based on two main variables: water temperature and volumetric flow rate, with temperatures ranging from 26ºC to 30ºC and flow rates from 4.5 m^3/h to 5.5 m^3/h.

As for the refrigerant, the temperature and the mass flow rate are characterized, both of which have been obtained thanks to the results provided by the compressor.

In conclusion, the modeling process is like that explained in the case of the evaporator, but introducing as data defined for the condenser.

To create the condenser component in TRNSYS, correlations and coefficients (Table 11) will be generated in MATLAB, with the results obtained in IMST-ART after the simulation of its behavior, for the total pressure drop (Δp_r) and for the condensing temperature (T_{ro}), the thermodynamic properties will be obtained through the CoolProp subroutine available in TRNSYS 18.

$$\Delta \mathrm{pr} = c_0 + c_1 * T_{seci} + c_2 * m_{seci} + c_3 \dot{m}_{ri} + c_4 T_{ri} + c_5 \dot{m}_{ri}^2$$

$$T_{ro} = c_0 + c_1 T_{seci} + c_2 m_{seci} + c_3 \dot{m}_{ri} + c_4 T_{ri} + c_5 m_{seci} \dot{m}_{ri} + c_6 m_{seci} T_{ri} + c_7 \dot{m}_{ri} T_{ri} + c_8 m_{seci} \dot{m}_{ri} T_{ri}$$

Table 11. Condenser coefficients

	T_{ro} [ºC]	Δp_r [Pa]
c_0	2.4904	15301
c_1	1.0005	-578.53
c_2	-0.054318	45.127
c_3	0.0099907	30.425
c_4	-0.023954	-35.944
c_5	-0.0010681	0.0434
c_6	0.00084235	
c_7	7.34E-05	
c_8	-3.76E-06	

The output variables are also the refrigerant outlet pressure, enthalpy and flow rate. The flow rate is kept constant, while the pressure and enthalpy are calculated using the CoolProp subroutine available in TRNSYS 18, assuming saturated liquid at the outlet.

7. Comparison under different operating conditions and selection of the best option.

In this section, two studies will be carried out. First, the COP and heating capacity will be analyzed considering different operating conditions. Then, the percentage of heat that can be used to heat domestic hot water will be evaluated.

Using the previously developed models, different operating conditions will be considered, taking into account the water temperature entering the condenser or gas cooler of the pool, the inlet air conditions, and different water flow rates. Table 12 shows the three water flow rates used: low ($\dot{m}_{w1}$), medium ($\dot{m}_{w3}$), and high ($\dot{m}_{w5}$).

Table 12. Water flow rates for R1234ze(E) and CO_2

	$\dot{m}_{w1}$ [kg/s]	$\dot{m}_{w3}$ [kg/s]	$\dot{m}_{w5}$ [kg/s]
R1234ze(E)	1.25	1.38	1.53
CO_2	1.45	1.61	1.77

Next, the influence of the three water flow rates on the COP for different water inlet temperatures to the condenser or gas cooler of the pool is analyzed, depending on the air temperature at the evaporator inlet.

Figure 12 shows the COP as a function of the air temperature for the mentioned flow rates, considering a water inlet temperature of 26ºC. Figure 12a presents results for the R1234ze(E) model, while Figure 12b shows the results for CO_2.

The same analysis is performed in the subsequent graphs for a water inlet temperature of 28°C (Figure 13) and 30°C (Figure 14).

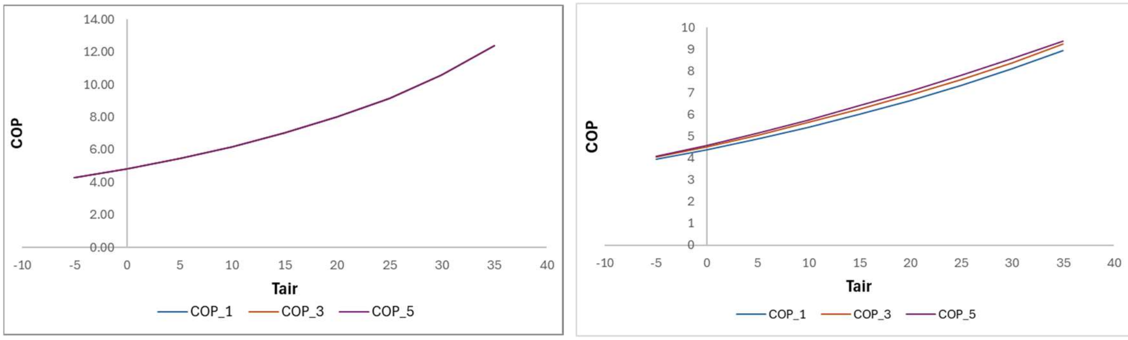

a) b)

Figure 12. Water temperature at 26 ºC at three different flow rates.

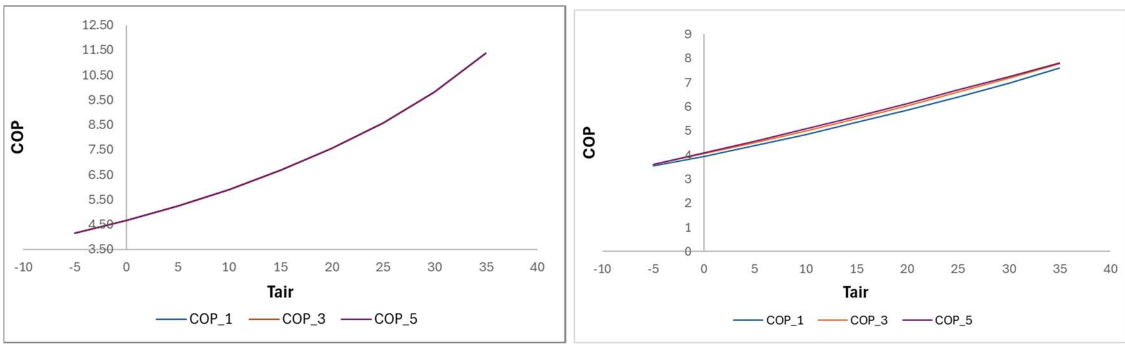

a) b)

Figure 13. Water temperature at 28 ºC at three different flow rates.

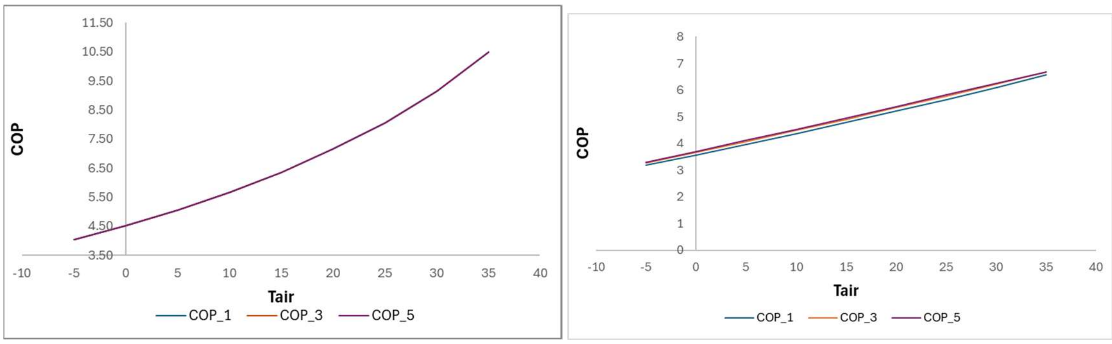

a) b)

Figure 14. Water temperature at 30 ºC at three different flow rates. As can be seen in the graphs, the difference in flow rate is hardly significant at the same water temperature, so we continue the study by analyzing the influence of the water temperature at the entrance of the condenser or gas cooler of the pool on the COP of the heat pump. For this, the average water flow rate estimated in Table 12 for each model has been considered, and the analysis has been performed for three water inlet temperatures (26ºC, 28ºC and 30ºC), depending on the air temperature at the evaporator inlet. It is observed (Figure 15) that the best results are obtained when the water temperature at the entrance is 26ºC, as this is when the highest COP is achieved.

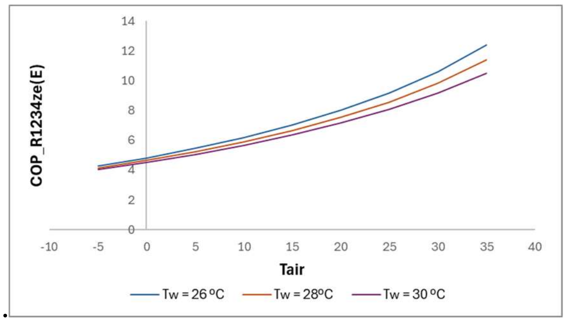

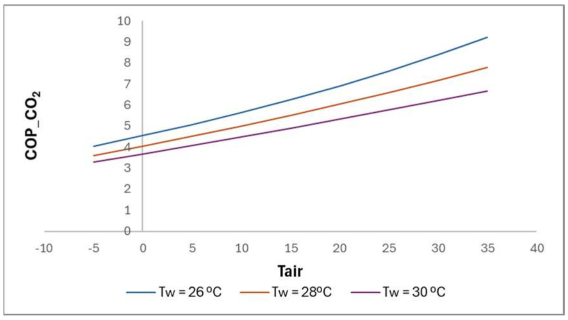

a) b)

Figure 15. Medium flow rate estimated at differents temperatures.

The influence of the inlet water flow rate on the heating capacity has also been studied, and we have found that, as with the COP, for a given temperature at different flow rates, there are hardly any significant differences.

Figure 16 analyzes the influence of the water temperature at the inlet of the condenser or the gas cooler of the pool on the heating capacity of both heat pumps. The heating capacity is represented as a function of the air temperature at the evaporator inlet, considering the average estimated water flow rate from Table 12 for each model and for three inlet water temperatures (26ºC, 28ºC and 30ºC).

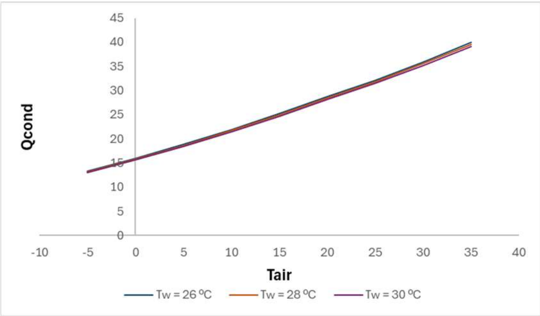

a)

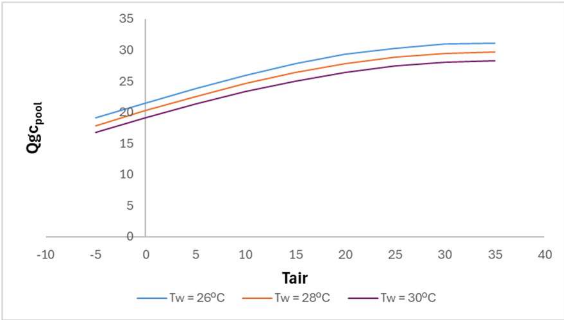

b)

Figure 16. Heating capacity at different temperatures.

Now we compare the heat pump model for the refrigerant R1234ze(E) and the model for CO2, for a water flow rate of 1.53 kg/s at a water temperature of 26 ºC we obtain the graphs of its COP and heating capacity in Figures 17 and 18, respectively.

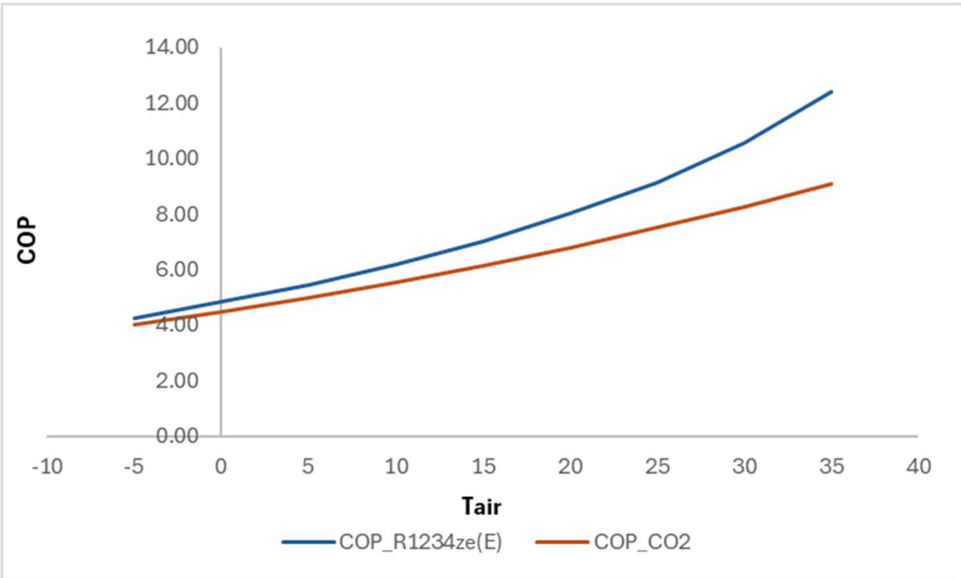

Figure 17. COP of both models

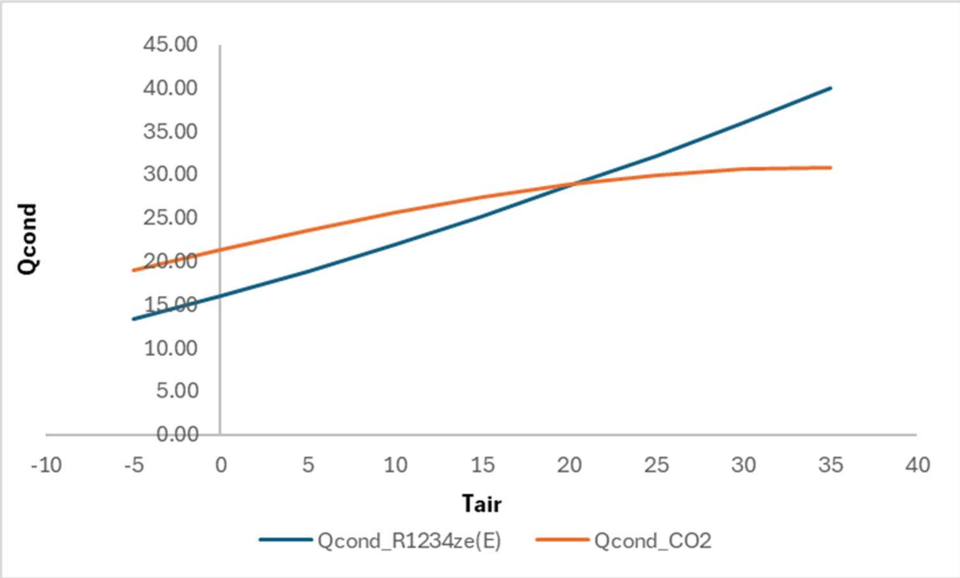

Figure 18. Heat capacity of both models

The graph in Figure 17 shows how the COP varies as a function of outdoor air temperature (T_{air}) for heat pumps with refrigerants R1234ze(E) and CO_2.

It can be observed that the heat pump with R1234ze(E) exhibits a higher COP than the one using CO_2 across the entire temperature range analyzed. This is because R1234ze(E) operates more efficiently under the same water flow and temperature conditions, thanks to its thermodynamic properties, such as a lower working pressure and a more favorable compression ratio. As the air temperature increases, the COP grows for both refrigerants, but the slope is steeper for R1234ze(E). This indicates that the heat pump with R1234ze(E) benefits more from higher ambient temperatures, making it particularly efficient in moderate or warm climates.

The heating capacity (Q_{cond}), which measures the amount of heat delivered to the system, also varies with outdoor air temperature. From the graph in Figure 18, it can be observed that CO_2 delivers higher heating capacity at lower temperatures. This can be attributed to CO_2's transcritical cycle behaviour, which allows it to deliver more heat even at low outdoor temperatures, making it ideal for cold climates.

However, as the outdoor air temperature increases, the heat capacity of the R1234ze(E) heat pump surpasses that of CO_2. This suggests that CO_2's performance stabilizes or slightly decreases at higher temperatures, possibly due to a smaller temperature gradient in the transcritical cycle. On the other hand, R1234ze(E), operating in a conventional subcritical cycle, continues to increase its heat delivery capacity as ambient temperature grows, making it more suitable for moderate or high temperatures.

Finally, a study is carried out to determine the percentage of heat that can be used to heat domestic hot water. To carry out this analysis, the developed CO_2 model has been employed. In the case of the R1234ze(E) refrigerant, the presence of a desuperheater has been considered, which reduces the refrigerant temperature from the compressor discharge conditions to 31 °C, assuming that the inlet water to the system has a temperature of 30 °C. This system exploits all the energy available in the refrigerant from its discharge at the compressor until it reaches 31 °C, assuming a thermal jump of 1 °C between the refrigerant and the water. We introduce the input data from Tables 13a and 13b into our models for R1234ze(E) and CO_2, respectively.

Table 13. Input data for models

a)

	R1234ze(E)
$\dot{m}_{W,in}$	1.53 kg/s
$T_{W,in}$	28 ºC

b)

	CO_2	
$\dot{m}_{gc,DHW}$	0.1 kg/s	0.3 kg/s
$T_{gc,DHW}$	30 ºC	
$\dot{m}_{gc,pool}$	0.9 kg/s	1.53 kg/s
$T_{gc,pool}$	28 ºC	

Considering the data from Table 13 and an air temperature of 15 °C, the percentage of heat that can be used to heat domestic hot water in the R1234ze(E) and CO_2 models can be observed in Table 14. To complete this study, a high flow rate ($\dot{m}_{gc,DHW,h}$) and a low flow rate ($\dot{m}_{gc,DHW,l}$) have been considered in the CO_2 model.

Table 14. Heat percentages for DHW

$T_{gc,DHW}$	R1234ze(E)	CO_2	
		$\dot{m}_{gc,DHW,l}$ = 0.1 [kg/s]	$\dot{m}_{gc,DHW,h}$ = 0.3 [kg/s]
10 ºC	100 %	100 %	100 %
20 ºC	100 %	100 %	100 %
30 ºC	**6.68 %**	**34.04 %**	**51.56 %**
40 ºC	0 %	20.19 %	28.75 %
50 ºC	0 %	7.58 %	8.32 %

As observed in Table 14, with the R1234ze(E) model, if the water enters at 10°C or 20°C, all the energy could be used to produce domestic hot water (DHW). However, if the water enters at 40°C or 50°C, no energy can be utilized, as the refrigerant condenses below these temperatures. When then inlet temperature is 30°C, only 6.68% of the total heat is allocated to domestic hot water, a considerably lower value compared to the CO_2 model.

On the other hand, CO_2, operating in a transcritical cycle, exhibits greater efficiency in heat transfer to DHW, especially at low to moderate temperatures. Additionally, increasing the water flow rate in the domestic hot water gas cooler (from 0.1 to 0.3) significantly improves the percentage of heat used for DHW, increasing from 34.04% to 51.56% for a water inlet temperature of 30°C. Figure 19 presents a graph illustrating these percentages for a DHW gas cooler water temperature of 30°C versus air temperature.

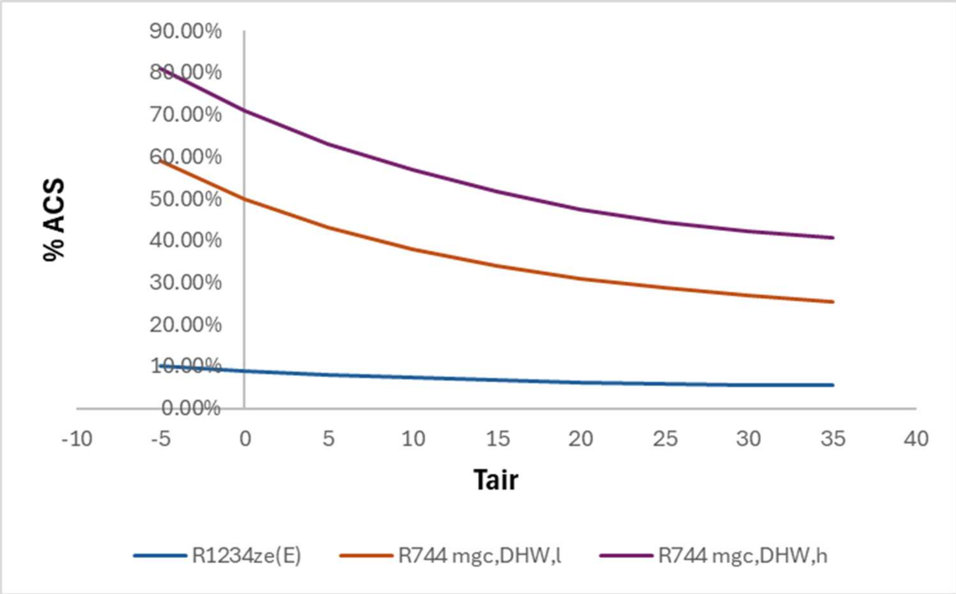

Figure 19. Comparasion of heat percentages for DHW

For a water temperature of 30ºC in the DHW gas cooler, the percentages obtained in the CO_2 model will be represented as a function of the water temperatures in the pool's gas cooler and the air temperature. The results are shown for a low water flow rate (Figure 20a) and for a high water flow rate (Figure 20b).

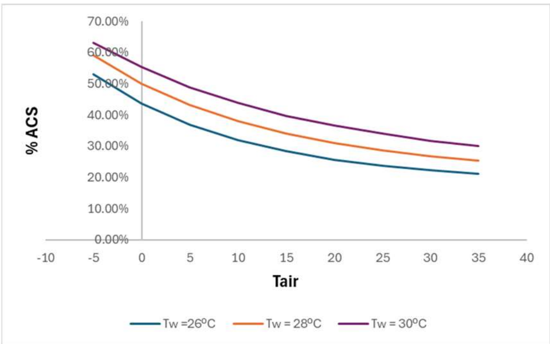

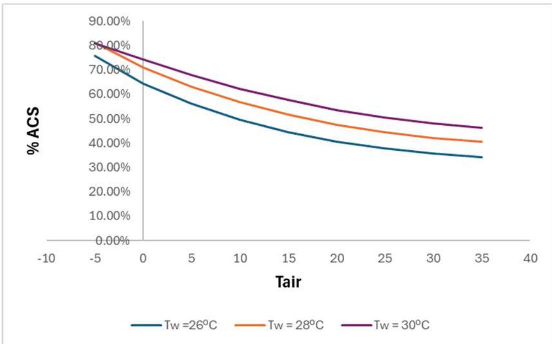

a) b)

Figure 20. Comparison of percentages in the CO_2 model

Figures 21a and 21b represent the same percentages obtained in the CO_2 model , but for a water temperature of 40ºC in the DHW gas cooler.

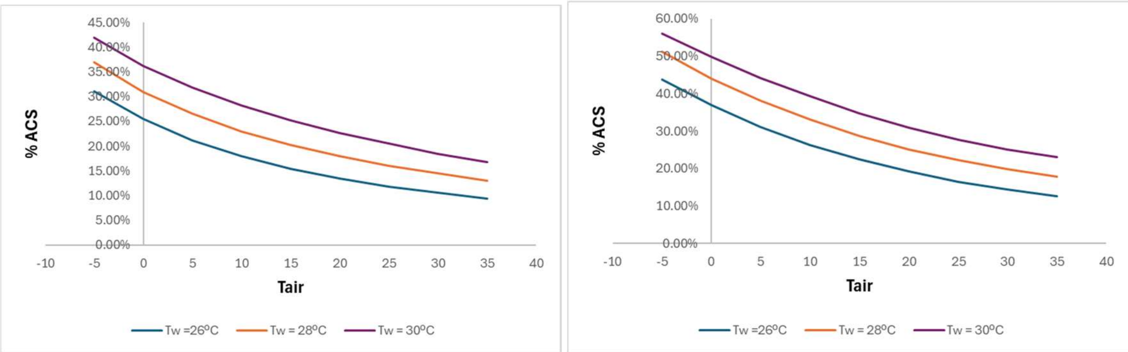

a) b)

Figure 21. Comparison of percentages in the CO_2 model

In Figures 22a and 22b, the same information is shown, but this time considering a water temperature of 50º C in the DHW gas cooler.

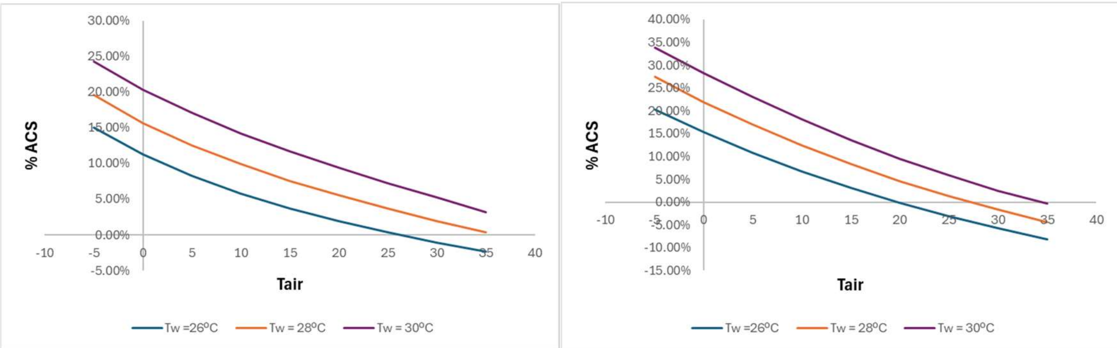

a) b)

Figure 22. Comparison of percentages in the CO_2 model

8. Conclusion

As a conclusion of this deliverable, basing the choice of refrigerant on the graphs from Figure 17 and Figure 18. This selection depends on the intended operating environment:

- R1234ze(E): It offers better overall performance in terms of efficiency (COP) and heating capacity in moderate to warm climates, making it more suitable for such conditions.
- CO_2: On the other hand, CO_2 is more efficient at lower temperatures and delivers higher heating capacity in these scenarios, making it ideal for applications in cold climates.

However, considering additional factors that influence refrigerant selection, such as global warming potential (GWP) and stability of heating capacity throughout the year, CO_2 presents key advantages. Despite R1234ze(E) showing a slightly higher COP, CO_2 has a much lower global warming potential and offers more consistent performance under ambient temperature variations, making it a more sustainable and practical solution in the long term. Moreover, as observed in Figure 19, the CO_2 model offers greater flexibility in combining pool heating with domestic hot water production.

9. Bibliography

https://www.bitzer.de/websoftware/

https://www.boe.es/buscar/pdf/2019/BOE-A-2019-15228-consolidado.pdf